Genome-wide RNAi screening identifies host restriction factors critical for in vivo AAV transduction

Miguel Mano[a,1], Rudy Ippodrino[a], Lorena Zentilin[a], Serena Zacchigna[a,b], and Mauro Giacca[a,b,1]

[a]Molecular Medicine Laboratory, International Centre for Genetic Engineering and Biotechnology, 34149 Trieste, Italy; and [b]Department of Medical, Surgical and Health Sciences, University of Trieste, Cattinara Hospital, 34149 Trieste, Italy

Edited by Kenneth I. Berns, University of Florida College of Medicine, Gainesville, FL, and approved July 29, 2015 (received for review February 20, 2015)

Viral vectors based on the adeno-associated virus (AAV) hold great promise for in vivo gene transfer; several unknowns, however, still limit the vectors' broader and more efficient application. Here, we report the results of a high-throughput, whole-genome siRNA screening aimed at identifying cellular factors regulating AAV transduction. We identified 1,483 genes affecting vector efficiency more than 4-fold and up to 50-fold, either negatively or positively. Most of these factors have not previously been associated to AAV infection. The most effective siRNAs were independent from the virus serotype or analyzed cell type and were equally evident for single-stranded and self-complementary AAV vectors. A common characteristic of the most effective siRNAs was the induction of cellular DNA damage and activation of a cell cycle checkpoint. This information can be exploited for the development of more efficient AAV-based gene delivery procedures. Administration of the most effective siRNAs identified by the screening to the liver significantly improved in vivo AAV transduction efficiency.

adeno-associated virus | DNA-damage response | high-throughput screening | self-complementary vectors | RNA interference

Viral vectors based on the adeno-associated virus (AAV) have received incremental attention over the past two decades as effective tools for in vivo gene transfer. The vectors' intrinsic structural simplicity, lack of pathogenicity, low immunogenicity, and ability to mediate long-term, episomal expression in nondividing cells in vitro and, most notably, postmitotic organs in vivo are desirable characteristics for several gene therapy applications (reviewed in ref. 1). Indeed, to date, over 90 clinical trials using these vectors have been carried out (www.abedia.com/wiley/index.html); the first commercial gene therapy product (Glybera) is an AAV1 vector for the treatment of familial lipoprotein lipase deficiency (2).

Despite these achievements, AAV vectors still display an undeniable number of limitations in terms of restricted cellular permissivity and efficacy of transgene expression. Efficient transduction in vivo is essentially limited to postmitotic cells [in particular, cardiomyocytes, neurons, retinal cells, and skeletal muscle fibers (1)] and requires infection at a relatively high multiplicity of infection; in addition, vector-driven gene expression is achieved only after a relatively long lag period (3). These characteristics are still incompletely understood in molecular terms but certainly reside within the intrinsic biological properties of target cells. This finding is also highlighted by the peculiar biology of wild-type AAV, which, for the completion of its biological cycle, requires cellular coinfection by adenovirus or other viruses that modify the cellular environment of the target cells, rendering them permissive for viral replication (4–6).

The efficient internalization of AAV vectors into different cell types is mediated by the binding of virions to ubiquitously expressed cell surface receptors (7, 8); tropism is further expanded by the availability of over a dozen different viral serotypes (9–12). Restriction of permissivity, however, mainly occurs at the postentry level, where multiple barriers constrain vector transduction. These include entrapment of virions inside the endosomal/lysosomal compartments, impaired nuclear translocation, and uncoating, inefficient single-stranded (ss) to double-stranded (ds) genome conversion and poor stabilization of newly formed viral dsDNA as single or concatemeric circular episomes (13–18). A better understanding of the cellular factors responsible for these molecular events appears crucial for the development of vectors capable of overcoming the limitations witnessed by a number of clinical applications (19–21).

Long-standing evidence hints at a specific connection between cellular stress and permissivity to AAV transduction. In particular, cell treatment with a variety of genotoxic agents or viral coinfection are major determinants of both wild-type AAV permissivity and efficiency of recombinant AAV vectors (reviewed in ref. 22). The molecular correlates of these observations, however, still remain vague.

Previous evidence had indicated that the conversion of the AAV ssDNA genome into a dsDNA form is a rate-limiting step for the onset of AAV-mediated transgene expression (13, 23). This has prompted the development of the self-complementary AAV (scAAV) vector technology, by which small AAV genomes, less than half the size of wild-type AAV, are efficiently packaged as dimeric inverted repeats (24).

To better understand the molecular determinants of AAV vector transduction and thus increase and expand their efficacy, here we report the results of a whole-genome, high-throughput siRNA screening, in which we assessed the effect of the knockdown of 18,120 human genes on AAV transduction. The siRNA technology represents a powerful tool to systematically investigate the role of cellular determinants on a given biological event and has already been applied to identify the host proteins needed for permissivity of different viruses, most notably HIV-1 (25, 26), hepatitis C virus (27), West Nile virus (28), and influenza virus (29).

By our screening, we identified 1,483 cellular factors significantly affecting, either positively or negatively, AAV vector efficiency. A common characteristic of the most effective siRNAs was the induction of cellular DNA damage. These findings are relevant for the development of innovative strategies to improve

Significance

Viral vectors based on the adeno-associated virus (AAV) are at the forefront of human gene therapy; yet, the molecular biology of these vectors is largely unexplored. The aim of this work was to unravel, in a systematic manner, the effect of the individual knockdown of over 18,000 human genes on the efficiency of AAV-mediated transduction. The results obtained connect AAV biology to the processing of cellular DNA damage and pave the way to practical applications to improve therapeutic gene transfer.

Author contributions: M.M., L.Z., and M.G. designed research; M.M., R.I., L.Z., and S.Z. performed research; M.M. and M.G. analyzed data; and M.M. and M.G. wrote the paper.

The authors declare no conflict of interest.

This article is a PNAS Direct Submission.

[1]To whom correspondence may be addressed. Email: giacca@icgeb.org or mano@icgeb.org.

This article contains supporting information online at www.pnas.org/lookup/suppl/doi:10.1073/pnas.1503607112/-/DCSupplemental.

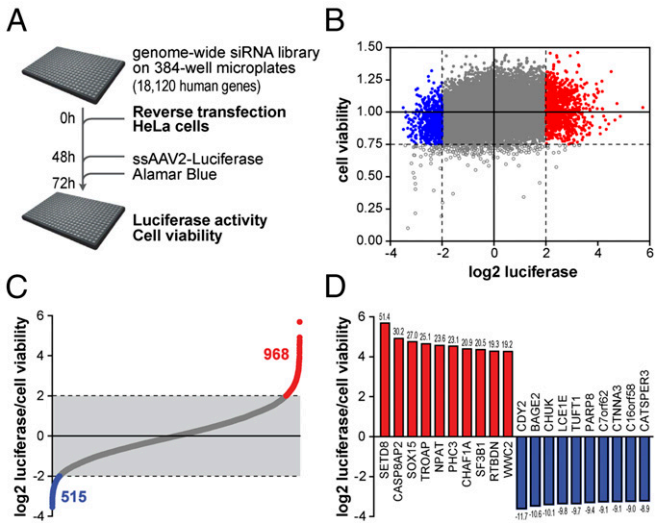

Fig. 1. Genome-wide RNAi screening identifies genes regulating AAV transduction. (*A*) Primary screening workflow. (*B*) Luciferase activity and cell viability after treatment with the siRNA library targeting 18,120 genes. siRNA pools increasing or decreasing AAV transduction by more than four-fold are highlighted in red and blue, respectively; siRNA pools decreasing cell viability to less than 75% (open circles) were excluded from further analysis. (*C*) Effect of siRNAs on AAV transduction; 968 genes were identified as negative regulators of AAV transduction and 515 as positive regulators. (*D*) Effect of the 10 most effective siRNA pools in increasing and decreasing AAV transduction. Numbers above and below bars represent fold changes. Averages from the two screening replicates are shown in *B*–*D*.

the efficiency of AAV transduction, either through the development of small molecules against the factors restricting AAV transduction or through their transient down-regulation. Indeed, the administration to the liver of the most effective siRNAs identified in the screening significantly improved AAV transduction efficiency.

Results

Genome-Wide RNAi Screening for AAV Permissivity. To systematically identify host cell factors that modulate the different steps of AAV transduction, we performed a high-throughput RNAi screening using a genome-wide siRNA library (18,120 human gene targets; pools of four siRNAs per gene arrayed on 384-well plates; Fig. 1*A*). HeLa cells were transfected with the siRNA library (>95% transfection efficiency; Fig. S1*A*) and 48 h later were infected with a recombinant ssAAV2 vector encoding the firefly luciferase reporter gene [ssAAV2-Luciferase; multiplicity of infection (moi): 2,500 viral genomes (vg)/cell]. Serotype 2 is the most common and more extensively studied AAV serotype. Luciferase activity was used to assess ssAAV2 transduction, and cell viability was monitored in parallel by using Alamar Blue. The screening was performed in duplicate; the replicates showed very good reproducibility [Spearman $r = 0.95$ (Fig. S1*B*); Fig. S1*C* shows controls].

This unbiased screening approach identified 1,483 genes affecting ssAAV2 transduction by more than fourfold (178 genes by more than eightfold). Of these, siRNAs targeting 968 genes increased ssAAV2 transduction (inhibitory genes; red in Fig. 1 *B* and *C* and Dataset S1), whereas siRNAs targeting 515 genes decreased ssAAV2 transduction by more than fourfold (required genes; blue in Fig. 1 *B* and *C* and Dataset S1). Of note, most of these genes have not been previously associated with ssAAV2 transduction. siRNA pools decreasing cell viability to less than 75% were considered toxic and were excluded from further analysis [256 of 18,120 siRNA pools (i.e., 1.4%); open circles in Fig. 1*B* and Dataset S1]; these included siRNAs against well known, essential genes [e.g., ubiquitin B and C, COPB1/2, polo-like kinase 1 (PLK1)]. Remarkably, the 10 top-scoring siRNA pools increased or decreased ssAAV2 transduction by as much as 50- and 10-fold, respectively (Fig. 1*D* and Table S1).

We wanted to confirm the results from the primary screening and discriminate between siRNAs targeting genes with a specific effect on ssAAV2 transduction from those with general effects on gene expression and/or protein production, which might thus indirectly affect AAV-encoded luciferase expression. We therefore performed a high-content fluorescence microscopy secondary screening using the siRNAs against the 1,483 genes that affected ssAAV2 transduction by more than fourfold in the primary screening. HeLa cells stably expressing EGFP (HeLa-EGFP) were transfected with the siRNAs of interest and transduced, 48 h later, with a ssAAV2 vector encoding the red fluorescent protein DsRed (ssAAV2-DsRed; moi: 2,500 vg/cell) (Fig. 2*A*). To eliminate any bias in the regulation of transgene expression, EGFP and DsRed reporter genes were expressed from analogous expression cassettes, driven by the cytomegalovirus immediate early (CMV IE) promoter.

From the 1,483 siRNA pools tested, we selected those that increased or decreased the percentage of DsRed-positive cells by

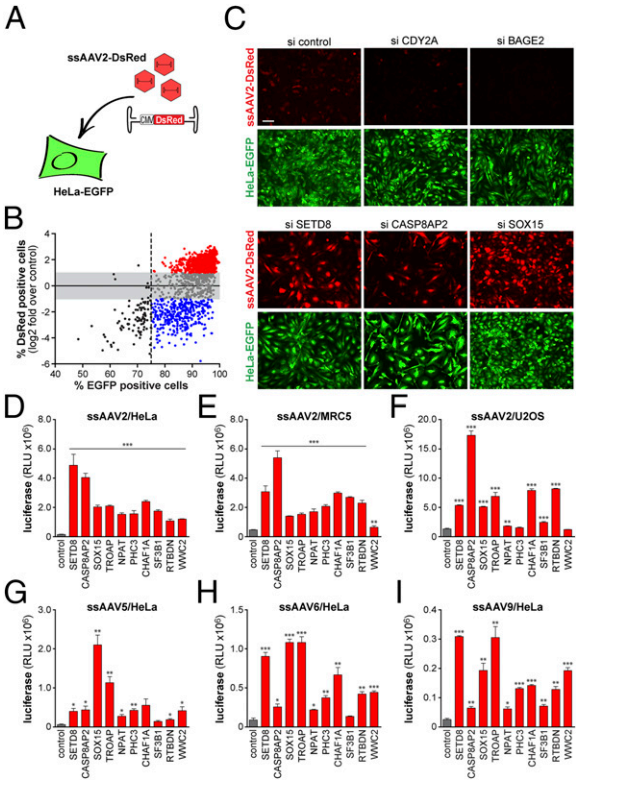

Fig. 2. Effect of siRNAs on AAV transduction is not cell-type specific and is independent of vector serotype. (*A*) Schematic of secondary high-content screening. (*B*) Percentage of DsRed- and EGFP-positive cells after treatment with siRNAs against the 1,483 genes selected from the primary screening. siRNA pools increasing or decreasing AAV transduction by more than two-fold are highlighted in red and blue, respectively; siRNA pools decreasing EGFP expression to less than 75% are shown in black. (*C*) Representative images of HeLa-EGFP cells treated with selected siRNA pools and transduced with ssAAV2-DsRed. (Scale bar: 100 μm.) (*D*–*I*) Effect of the 10 siRNA pools that increased AAV transduction more efficiently in the primary screening, in three different cell lines [HeLa (*D*), MRC5 (*E*), and U2OS (*F*)] and using three different AAV serotypes in HeLa cells [AAV5 (*G*), AAV6 (*H*), and AAV9 (*I*)]; results are shown as means ± SEM [$n = 4$ (*D*–*F*); $n = 3$ (*G*–*I*)]. $^*P < 0.05$, $^{**}P < 0.01$, and $^{***}P < 0.001$ of individual datasets vs. control.

CELL BIOLOGY

more than twofold, compared with control siRNA (red and blue, respectively, in Fig. 2*B*; Dataset S2). The siRNAs that resulted in less than 75% EGFP-positive cells were removed from our candidate list (95 of 1,483 siRNA pools; black in Fig. 2*B*; Dataset S2). This two-step screening procedure resulted in a final candidate list composed of 710 genes inhibitory of, and 414 genes required for, efficient ssAAV2 transduction. Representative images of cells treated with the control siRNA or siRNAs that decrease [against chromodomain protein, Y-linked, 2A (CDY2A); and B melanoma antigen family, member 2 (BAGE2)] or increase [against SET domain-containing (lysine methyltransferase) 8 (SETD8); caspase 8-associated protein 2 (CASP8AP2); and SRY (sex-determining region Y)-box 15 (SOX15)] ssAAV2 transduction are shown in Fig. 2*C*; results for the top 10 genes are shown in Fig. S2. Gene-ontology analysis of the genes inhibiting ssAAV2 transduction revealed a clear overrepresentation of genes related to cell cycle, cellular growth and proliferation, and DNA recombination and repair, whereas in the subset of genes required for transduction an overrepresentation of genes involved in gene expression, intracellular trafficking and transcription was observed (Fig. S3 *A* and *B*).

The use of pooled siRNA libraries (here four siRNAs per gene) decreases the likelihood of off-target effects by lowering the effective concentration of each individual siRNA. To test the efficacy of the individual siRNAs in each pool, we deconvoluted the siRNA pools corresponding to the 108 top candidate genes of the primary screening (68 inhibitory genes and 40 required genes) and assessed the effect of each siRNA on ssAAV2 transduction (432 siRNAs total). Overall, 78 of the 108 tested genes (72%) were validated, each one with at least two siRNAs exhibiting a phenotype matching that of the corresponding pool (Fig. S4). The top 10 genes increasing ssAAV2 transduction were all successfully validated using this criterion (Fig. S4).

Given our interest in improving AAV2 transduction for gene transfer applications, we concentrated on the top 10 genes that, once silenced, increase ssAAV2 efficiency (i.e., act as inhibitors of viral transduction). The effect of these genes was not restricted to HeLa cells but could also be observed in two other human cell lines (U2OS and MRC5; Fig. 2 *D–F*). The effect of the top 10 most effective siRNAs was also observed in HeLa cell transduction by other AAV serotypes (AAV5, AAV6, AAV9; Fig. 2 *G–I*). Efficient knockdown of the top 10-selected genes was verified (Fig. S5). Of note, silencing of these genes also increased transduction of ΔVP1-ssAAV2 particles, which are strongly impaired in intracellular trafficking (30). However, transduction was significantly lower than that of wild-type AAV vectors (Fig. S6; compare Fig. 2*D*). Together, these findings indicate that the identified genes are broad regulators of ssAAV transduction, irrespective of target cells or vector serotype.

A Largely Overlapping Set of Host Factors Regulates both ssAAV and scAAV Transduction. scAAV vectors have gained increased attention because of their higher efficiency of transduction of several tissues in vivo. We performed an additional high-content microscopy secondary screening to compare the cellular factors required for transduction by ssAAV and scAAV vectors. Cells were transfected with siRNAs targeting the 1,483 genes selected from the primary screening, and, 48 h after cells were transduced with an scAAV2 vector encoding EGFP (scAAV2-EGFP; moi: 2,500 vg/cell) (Fig. 3*A*). There was remarkable correlation between the ss- and scAAV2 results (Spearman $r = 0.84$; Fig. 3*B* and Dataset S3), indicating that most of the identified effects were common for both vectors. Notwithstanding this communality, some siRNAs showed a differential effect (130 genes showing a >twofold difference in their effect on ss- compared with scAAV vectors; 8.8%). Among others, the siRNAs against P2RX7 preferentially increased ssAAV transduction, whereas the siRNAs against SAE1 preferentially increased scAAV transduction (Fig. 3 *B* and *C* and Dataset S3). Of note, the top 10 siRNA pools described above for ssAAV2 vectors increased transduction of scAAV2 to a similar extent (Fig. 3*D* and Dataset S3).

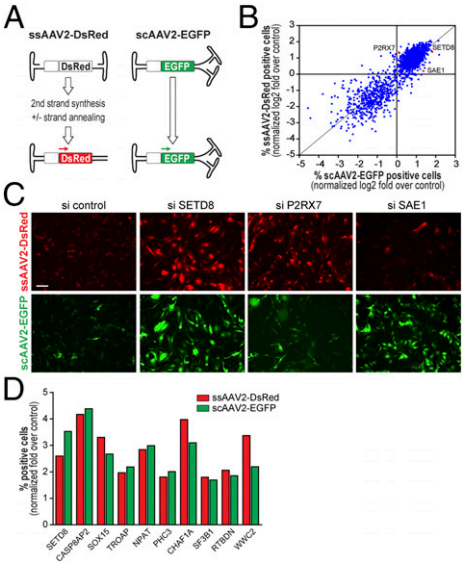

Fig. 3. Transduction by ssAAV and scAAV is controlled by an overlapping set of host factors. (*A*) Schematic of ssAAV2-DsRed and scAAV2-EGFP. (*B*) Analysis of cellular factors required for transduction by ssAAV and scAAV vectors. siRNAs against the 1,483 genes selected from the primary screening were tested. (*C*) Representative images of HeLa cells treated with control or selected siRNAs (SETD8, P2RX7, and SAE1) and transduced with ssAAV2-DsRed or scAAV2-EGFP. (Scale bar: 100 μm.) (*D*) Effect of top 10 siRNAs increasing AAV transduction, selected based on the primary screening, on ssAAV2-DsRed and scAAV2-EGFP transduction. Averages from the two screening replicates are shown in *B* and *D*.

Cellular DNA Damage Is a Strong Determinant of AAV Transduction. Long-standing evidence indicates that genotoxic damage is a major determinant of cellular permissivity to AAV (4, 5). In addition, AAV transduction is inhibited by proteins of the DNA-damage response (DDR) (31), in both cell culture (32) and in vivo (33). Finally, among the genes inhibitory to ssAAV2 transduction in our primary screening, there was a clear overrepresentation of functional gene categories related to cellular growth and proliferation, cell cycle, and DNA repair (Fig. S3). These observations prompted us to investigate the effect of the siRNAs identified to regulate AAV permissivity on cellular DNA damage, in the absence of viral infection.

We performed an additional image-based screening to investigate the effect of the 968 siRNA pools increasing ssAAV transduction and of the 515 siRNA pools decreasing it, on the phosphorylation of histone H2AX at serine 139 (γ-H2AX), a hallmark of cellular DNA damage. We found that 17 of 968 and 2 of 515 siRNAs also determined the formation of γ-H2AX foci ($P < 0.05$; Fig. 4*A* and Dataset S4). Even more remarkably, if one considers the top 10 most effective and the top 10 least effective siRNAs, 5 of 10 and 0 of 10, respectively, also determine DNA damage ($P < 0.01$; Fig. 4*B*). Down-regulation of all these genes also induced a remarkable aberration of the cell cycle profile, suggesting cell cycle checkpoint activation (Fig. 4*C*). In a consistent manner, the siRNAs against these five genes also induced phosphorylation of CHK1; in the case of SETD8 and CASP8AP2, phosphorylation of ATM was also observed (Fig. 4*D*). Hydroxyurea (HU) was used a positive control in these experiments.

These results indicate that several of the siRNAs inducing cellular permissivity to AAV also determine DNA damage. This

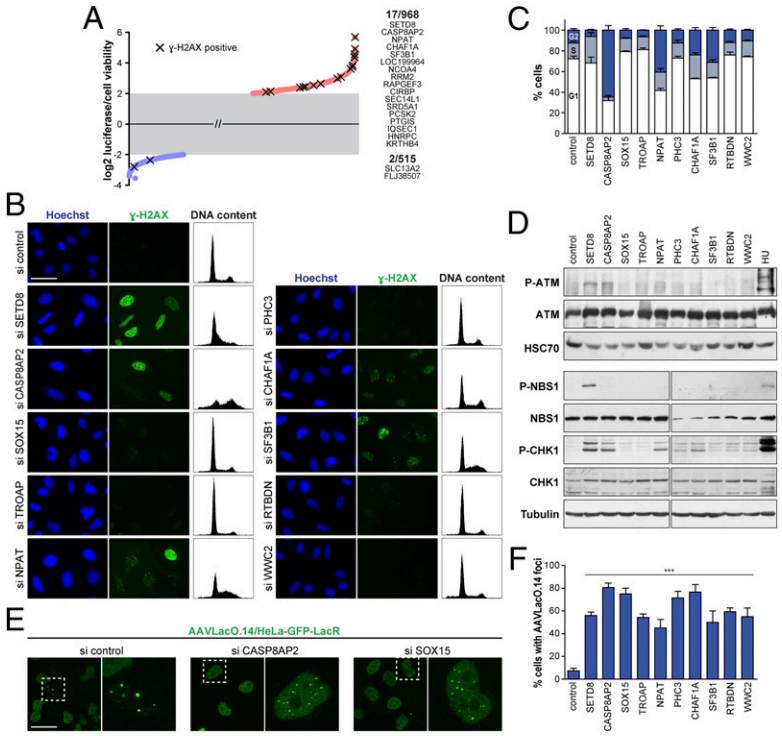

Fig. 4. Cellular DNA damage is a major determinant of AAV transduction. (*A*) Effect of knockdown of genes affecting AAV transduction on cellular DNA damage, detected by the presence of γ-H2AX foci. siRNA pools targeting the 1,483 genes selected from the primary screening were tested; 17 of the 968 genes identified as negative regulators of AAV transduction and 2 of the 515 genes identified as positive regulators induced γ-H2AX foci (marked with crosses in the graph). (*B*) Effect of the top 10 selected siRNAs on cellular DNA damage and cell cycle (*Right*). (Scale bar: 50 μm.) (*C*) Percentage of HeLa cells in the different stages of the cell cycle, following treatment with the top 10 siRNA pools; results are shown as means ± SEM ($n = 3$). Cells treated with siRNAs against SETD8, CASP8AP2, NPAT, CHAF1A, and SF3B1 are significantly different compared with control ($P < 0.01$). (*D*) Western blot for proteins involved in different steps of the cellular DDR pathways, following treatment with the top 10 siRNA pools. (*E*) Representative images of cells showing nuclear GFP-LacR foci after treatment with control siRNA or siRNAs targeting CASP8AP2 and SOX15. (Scale bar: 50 μm.) (*F*) Percentage of HeLa cells presenting GFP-LacR nuclear foci, following treatment with the top 10 siRNA pools. GFP-LacR foci correlate with efficient ssAAV to dsAAV genome conversion. Results are shown as means ± SEM ($n = 3$). ***$P < 0.001$.

conclusion is consistent with our previous observation showing that DDR activation reduces binding of cellular DNA-damage sensing proteins, including MRN (Mre11, Rad50, Nbs1) members, to the incoming AAV genomes, thus facilitating their ss- to dsDNA conversion (32, 33). We also analyzed the extent of ss- to dsDNA conversion using a cellular system based on the visualization of dsDNA AAV genomes carrying multiple repeats of the Lac operator sequence, in HeLa cells expressing a nuclear Lac repressor (32). We found that all of the top 10 siRNAs increased the percentage of cells carrying dsDNA AAV foci in the nucleus (Fig. 4 *E* and *F*).

Transient Knockdown of the Identified Inhibitory Genes Boosts AAV Transduction in Vivo. Finally, we wanted to assess whether knockdown of the inhibitory genes identified in the screening might also improve AAV transduction in vivo. siRNA pools targeting the mouse orthologs of the top 10 inhibitory genes, formulated with a commercial cationic lipid-based transfection reagent, were administered to 1-mo-old mice by portal vein injection together with an ssAAV8 vector encoding EGFP (ssAAV8-ApoE/hAAT-EGFP; 5×10^{10} vg; Fig. 5*A*). Serotype 8 was selected for its superior performance in the liver compared with AAV2 (3, 34); EGFP expression was driven by the ApoE/hAAT promoter, which does not undergo transcriptional silencing over time in the liver (35). Analysis of liver EGFP fluorescence at 10 d after injection indicated a significant increase in the levels of transduction of the ssAAV8-ApoE/hAAT-EGFP vector, when coinjected with siRNAs against the top 10 inhibitory genes (Fig. 5 *B* and *C* and Fig. S7). This increase in transduction was widespread throughout the liver, in particular, in the pericentral vein areas, which are common AAV8 transduction target regions following portal injection in mice (36) (Fig. 5*B* and Fig. S7). Real-time, quantitative (q)RT-PCR quantification of the levels of EGFP mRNA correlated with the extent of EGFP expression in the analyzed livers (Fig. 5 *C* and *D*).

The effect of siRNAs against two genes that induce DNA damage (SETD8 and CASP8AP2) and three genes that have no implications on DNA damage [trophinin-associated protein (tastin) (TROAP), polyhomeotic homolog 3 (*Drosophila*) (PHC3), and Retbindin (RTBDN)] was also analyzed at 5 wk after injection. A significant increase of AAV transduction was also observed at this time point (Fig. 5 *E* and *F* and Fig. S8), indicating stable AAV transduction. Of note, the siRNA sequences used for these in vivo experiments were designed to target the mouse orthologs of the top 10 inhibitory genes. Efficacy of the mouse siRNAs further confirms the specificity of the observed effects and the inhibitory function of the identified genes on AAV transduction.

Discussion

Viral vectors based on AAV have gained increasing popularity because of several favorable characteristics, including an excellent safety profile, no inflammatory response, prolonged transgene expression, relative genetic simplicity, and high efficiency of transduction of postmitotic tissues in vivo. Nonetheless, it has become evident that significant improvements need to be achieved before attaining broader clinical application. Given the molecular simplicity of AAV vector particles, all of the determinants of permissivity to vector transduction appear to reside among the molecular features of the host cell.

To our knowledge, this study is the first to address this issue on a genome-wide scale, using an unbiased RNAi screening strategy (18,120 human target genes). By performing a systematic high-throughput siRNA primary screening based on luciferase gene expression, followed by an image-based secondary screening to quantify the fraction of AAV-transduced cells, we identified two sets of genes with a strong effect on AAV2 transduction, including 710 negative and 414 positive regulators. The fact that the top 10 genes that restrict AAV2 transduction are also active on other serotypes indicates that the major processes restricting AAV transduction are most likely subsequent to cell attachment and vector entry.

The number of cellular factors restricting AAV transduction was unexpectedly high (1124, 6.2%). Additionally, there was no apparent homogeneity of function among these factors, except that most fitted into the categories related to cell cycle regulation

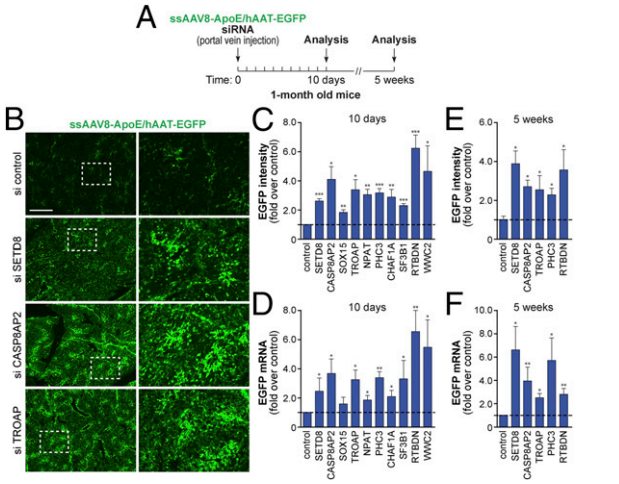

Fig. 5. Knockdown of the identified inhibitory genes improves AAV transduction in vivo. (*A*) Schematic of the in vivo AAV transduction experiments. (*B*) Representative images of liver sections of animals treated with control and selected siRNAs and transduced with AAV8 encoding EGFP (ssAAV8-ApoE/hAAT-EGFP). siRNA pools formulated with a commercial transfection reagent were delivered together with ssAAV8-ApoE/hAAT-EGFP by portal vein injection and analyzed 10 d after injection. (Scale bar: 1 mm.) (*C* and *E*) EGFP fluorescence intensity levels in tissue samples analyzed at 10 d (*C*) or 5 wk (*E*) after injection. (*D* and *F*) EGFP mRNA levels in tissue samples, quantified by qRT-PCR at 10 d (*D*) or 5 wk (*F*) after injection. Results in *C*–*F* are shown as means ± SEM ($n = 3$). $*P < 0.05$, $**P < 0.01$, and $***P < 0.001$.

and DNA recombination and repair. Of the five proteins affected by the most effective siRNAs, SETD8 is a SET domain containing lysine methyltransferase (37), CASP8AP2 is a component of the apoptotic machinery (38), SOX15 is a developmental transcription factor (39), TROAP is a cell adhesion molecule reported to mediate blastocyst implantation (40), and NPAT is a cell cycle progression regulator encoded within the ATM gene (41). This heterogeneity of function might indicate that AAV transduction is regulated at multiple levels or that, more likely, the knockdown of these factors converge into common intracellular signaling pathways. Indeed, we observed that several of the siRNAs inducing AAV transduction also directly induced cellular DNA damage and checkpoint activation (in particular, 5 of the top 10 most effective in increasing AAV transduction).

We previously reported that proteins sensing DNA damage, in particular, the members of the MRN complex and MDC1, restrict AAV transduction by directly binding the incoming AAV genomes (32, 42). Down-regulation of these proteins, as it occurs along terminal cell differentiation or following RNAi, positively correlates with increased AAV permissivity both in vitro and in vivo (33). Based on this evidence, we proposed a model by which the induction of cellular DNA damage titrates MRN and other components of the DDR away from the AAV genomes, thus allowing their proper processing (32). This "titration model" explains well why the induction of cellular DNA damage, through treatment of cells with genotoxic agents (e.g., HU, UV radiation), favors AAV transduction in vitro and in vivo (4, 5). The current observation that, among the most effective genes restricting AAV transduction, there is a clear overrepresentation of genes that once depleted lead to cellular DNA damage is fully consistent with this model. Importantly, the top-scoring genes inducing DNA damage and AAV transduction [SETD8; CASP8AP2; NPAT; chromatin assembly factor 1, subunit A (p150) (CHAF1A); and WW and C2 domain-containing 2 (WWC2)] act on different cellular processes and have no direct function on the DDR pathways.

We also observed a strong correlation between the genes acting as positive or negative regulators of ssAAV and scAAV vectors. This suggests that, although scAAV vectors have the capacity to self-anneal and thus produce ds transcriptional units more efficiently than conventional ssAAV vectors (24), the major determinants of transduction appear to impact on other steps of vector processing; the fact that the genome structure of scAAV and ssAAV are identical [inverted terminal repeats (ITRs) and ss–ds junctions at the hairpins are retained] may explain similarities in genome processing and justify the observed correlation. Consistent with this conclusion, recent evidence indicates that scAAVs are still inhibited by MRN (43), again suggesting that physical interaction of the vector DNA with the cellular DDR machinery is a major restriction factor for transduction. In this respect, however, a caveat is that in our experiments, the selection of candidate genes for scAAV vectors was performed based on the results of the initial screenings performed with ssAAV vectors. Thus, we cannot formally exclude the existence of genes that may have very prominent effects on scAAV while not affecting ssAAV transduction and have thus escaped detection in our primary screening.

An RNAi screening aimed at identifying cellular proteins controlling AAV2 transduction was performed previously by Wallen et al. in human aortic endothelial cells, using a siRNA library targeting 5,520 genes (Druggable Genome Library; pools of three siRNAs per gene) (44). This screening was dominated by off-target effects (four of the top five siRNAs were attributed to seed sequence off-targets), rendering the comparison of results with our study difficult. siRNA library design algorithms, pooling strategy, and assay conditions are certainly important factors that contributed to these results; of note, the seed sequence identified by the authors (nucleotides 2–7; 5′-UGUUUC-3′) was present in only 1 of the 72,480 siRNAs tested in our study. In our work, we validated approximately 70% of the 108 tested candidate genes in deconvolution experiments, with at least two of the four individual siRNAs tested for each gene recapitulating the phenotype of the siRNA pools. In particular, we validated the top 10 genes increasing AAV transduction by both deconvolution experiments and using different sets of siRNAs designed to target the mouse orthologs of these 10 genes in vivo. These results argue in favor of a high degree of confidence in the genes identified in this study.

The observation that the siRNAs targeting each of the top 10 inhibitory genes markedly increased AAV liver transduction has potential translational value, because it provides proof-of-principle that RNAi and, presumably, pharmacological modulation of the factors identified through this functional genomics approach can be successfully exploited to improve AAV efficiency in vivo. The liver itself is an important organ for AAV-targeted applications, including gene therapy of hemophilia (45) and of various other inherited disorders (46–48).

In closing, data from this comprehensive large-scale study constitutes a useful resource to further dissect the molecular aspects of AAV biology and to design strategies aimed at improving the utilization of AAV vectors in the gene therapy arena.

Materials and Methods

Production and Purification of Recombinant AAV Vectors. All of the AAV vectors used in this study were generated by the International Centre for Genetic Engineering and Biotechnology (ICGEB) AAV Vector Unit (AVU) (www.icgeb.org/avu-core-facility.html) using a dual/triple plasmid cotransfection procedure followed by PEG precipitation and purification through $CsCl_2$ gradient centrifugations.

Genome-Wide RNAi Screening. The genome-wide human siRNA library (siGENOME SMARTPool; pools of four siRNAs per gene) targeting 18,120 human genes was obtained from Dharmacon, Thermo Scientific (catalog no. G-005005). The siRNA library, arrayed on 384-well plates, was transfected into HeLa cells using a standard reverse transfection protocol, at a final siRNA

concentration of 50 nM. Forty-eight hours after transfection, cells were transduced with a recombinant ssAAV2 vector (ssAAV2-Luciferase; moi: 2,500 vg/cell) encoding for the Firefly luciferase reporter gene; 21 h later, Alamar Blue (Life Technologies) was added to the culture medium for 3 h. Luciferase activity (AAV transduction) and cell viability were measure at 72 h after transfection. For the image-based secondary, siRNA pools were "cherry-picked" from the genome-wide siRNA library. Image acquisition and analysis was performed using an ImageXpress Micro automated high-content screening fluorescence microscope and MetaXpress software (Molecular Devices). All screenings were performed in duplicate at the ICGEB High-Throughput Screening Facility (www.icgeb.org/high-throughput-screening.html).

AAV Liver Transduction. CD1 mice were purchased from Charles River Laboratories Italia Srl. Animal care and treatments were conducted in conformity with institutional guidelines in compliance with national and international laws and policies (European Economic Community Council Directive 86/609, Official Journal L 358, 12 December 1987). Juvenile mice (CD1; 1-mo old; n = 3–5 per group) were injected into the portal vein with a mixture of transfection reagent (Lipofectamine RNAiMAX) and siRNAs, together with AAV8-ApoE/hAAT-EGFP (5×10^{10} vg). Animals were killed 10 d or 5 wk after injection, and livers were analyzed for the percentage of transduced cells by fluorescent microscopy, or quantification of EGFP expression, by real-time qPCR.

Detailed procedures and associated references are available in *SI Materials and Methods*.

ACKNOWLEDGMENTS. We thank Marina Dapas and Michela Zotti for technical support in AAV production, J. A. Kleinschmidt for providing a ΔVP1-AAV plasmid, and Suzanne Kerbavcic for editorial assistance. M.M. is supported by the Fondo per gli Investimenti della Ricerca di Base RBAP11Z4Z9 project of the Ministero dell'Istruzione, dell'Università e della Ricerca, Italy. R.I. is supported by an ICGEB Arturo Falaschi Pre-Doctoral Fellowship. This work was supported by Telethon Foundation Grant GGP11068, Italy, and European Research Council Advanced Grant 250124 (to M.G.).

1. Zacchigna S, Zentilin L, Giacca M (2014) Adeno-associated virus vectors as therapeutic and investigational tools in the cardiovascular system. *Circ Res* 114(11):1827–1846.
2. Flotte TR (2013) Birth of a new therapeutic platform: 47 years of adeno-associated virus biology from virus discovery to licensed gene therapy. *Mol Ther* 21(11): 1976–1981.
3. Zincarelli C, Soltys S, Rengo G, Rabinowitz JE (2008) Analysis of AAV serotypes 1-9 mediated gene expression and tropism in mice after systemic injection. *Mol Ther* 16(6):1073–1080.
4. Berns KI, Linden RM (1995) The cryptic life style of adeno-associated virus. *BioEssays* 17(3):237–245.
5. Carter BJ (2004) Adeno-associated virus and the development of adeno-associated virus vectors: A historical perspective. *Mol Ther* 10(6):981–989.
6. Geoffroy MC, Salvetti A (2005) Helper functions required for wild type and recombinant adeno-associated virus growth. *Curr Gene Ther* 5(3):265–271.
7. Wu Z, Asokan A, Samulski RJ (2006) Adeno-associated virus serotypes: Vector toolkit for human gene therapy. *Mol Ther* 14(3):316–327.
8. Shen S, Bryant KD, Brown SM, Randell SH, Asokan A (2011) Terminal N-linked galactose is the primary receptor for adeno-associated virus 9. *J Biol Chem* 286(15): 13532–13540.
9. Gao G, Vandenberghe LH, Wilson JM (2005) New recombinant serotypes of AAV vectors. *Curr Gene Ther* 5(3):285–297.
10. Agbandje-McKenna M, Kleinschmidt J (2011) AAV capsid structure and cell interactions. *Methods Mol Biol* 807:47–92.
11. Mietzsch M, Broecker F, Reinhardt A, Seeberger PH, Heilbronn R (2014) Differential adeno-associated virus serotype-specific interaction patterns with synthetic heparins and other glycans. *J Virol* 88(5):2991–3003.
12. Vandenberghe LH, Wilson JM, Gao G (2009) Tailoring the AAV vector capsid for gene therapy. *Gene Ther* 16(3):311–319.
13. Fisher KJ, et al. (1996) Transduction with recombinant adeno-associated virus for gene therapy is limited by leading-strand synthesis. *J Virol* 70(1):520–532.
14. Xiao PJ, Samulski RJ (2012) Cytoplasmic trafficking, endosomal escape, and perinuclear accumulation of adeno-associated virus type 2 particles are facilitated by microtubule network. *J Virol* 86(19):10462–10473.
15. Choi VW, McCarty DM, Samulski RJ (2006) Host cell DNA repair pathways in adeno-associated viral genome processing. *J Virol* 80(21):10346–10356.
16. Xiao W, Warrington KH, Jr, Hearing P, Hughes J, Muzyczka N (2002) Adenovirus-facilitated nuclear translocation of adeno-associated virus type 2. *J Virol* 76(22): 11505–11517.
17. Nakai H, Storm TA, Kay MA (2000) Recruitment of single-stranded recombinant adeno-associated virus vector genomes and intermolecular recombination are responsible for stable transduction of liver in vivo. *J Virol* 74(20):9451–9463.
18. Yang J, et al. (1999) Concatamerization of adeno-associated virus circular genomes occurs through intermolecular recombination. *J Virol* 73(11):9468–9477.
19. Manno CS, et al. (2006) Successful transduction of liver in hemophilia by AAV-Factor IX and limitations imposed by the host immune response. *Nat Med* 12(3):342–347.
20. Hasbrouck NC, High KA (2008) AAV-mediated gene transfer for the treatment of hemophilia B: Problems and prospects. *Gene Ther* 15(11):870–875.
21. Moss RB, et al. (2007) Repeated aerosolized AAV-CFTR for treatment of cystic fibrosis: A randomized placebo-controlled phase 2B trial. *Hum Gene Ther* 18(8):726–732.
22. Weitzman MD, Carson CT, Schwartz RA, Lilley CE (2004) Interactions of viruses with the cellular DNA repair machinery. *DNA Repair (Amst)* 3(8-9):1165–1173.
23. Ferrari FK, Samulski T, Shenk T, Samulski RJ (1996) Second-strand synthesis is a rate-limiting step for efficient transduction by recombinant adeno-associated virus vectors. *J Virol* 70(5):3227–3234.
24. McCarty DM, Monahan PE, Samulski RJ (2001) Self-complementary recombinant adeno-associated virus (scAAV) vectors promote efficient transduction independently of DNA synthesis. *Gene Ther* 8(16):1248–1254.
25. Brass AL, et al. (2008) Identification of host proteins required for HIV infection through a functional genomic screen. *Science* 319(5865):921–926.
26. König R, et al. (2008) Global analysis of host-pathogen interactions that regulate early-stage HIV-1 replication. *Cell* 135(1):49–60.
27. Li Q, et al. (2009) A genome-wide genetic screen for host factors required for hepatitis C virus propagation. *Proc Natl Acad Sci USA* 106(38):16410–16415.
28. Krishnan MN, et al. (2008) RNA interference screen for human genes associated with West Nile virus infection. *Nature* 455(7210):242–245.
29. Karlas A, et al. (2010) Genome-wide RNAi screen identifies human host factors crucial for influenza virus replication. *Nature* 463(7282):818–822.
30. Popa-Wagner R, et al. (2012) Impact of VP1-specific protein sequence motifs on adeno-associated virus type 2 intracellular trafficking and nuclear entry. *J Virol* 86(17): 9163–9174.
31. Zentilin L, Marcello A, Giacca M (2001) Involvement of cellular double-stranded DNA break binding proteins in processing of the recombinant adeno-associated virus genome. *J Virol* 75(24):12279–12287.
32. Cervelli T, et al. (2008) Processing of recombinant AAV genomes occurs in specific nuclear structures that overlap with foci of DNA-damage-response proteins. *J Cell Sci* 121(Pt 3):349–357.
33. Lovric J, et al. (2012) Terminal differentiation of cardiac and skeletal myocytes induces permissivity to AAV transduction by relieving inhibition imposed by DNA damage response proteins. *Mol Ther* 20(11):2087–2097.
34. Vandendriessche T, et al. (2007) Efficacy and safety of adeno-associated viral vectors based on serotype 8 and 9 vs. lentiviral vectors for hemophilia B gene therapy. *J Thromb Haemost* 5(1):16–24.
35. Okuyama T, et al. (1996) Liver-directed gene therapy: A retroviral vector with a complete LTR and the ApoE enhancer-alpha 1-antitrypsin promoter dramatically increases expression of human alpha 1-antitrypsin in vivo. *Hum Gene Ther* 7(5):637–645.
36. Bell P, et al. (2011) Inverse zonation of hepatocyte transduction with AAV vectors between mice and non-human primates. *Mol Genet Metab* 104(3):395–403.
37. Fang J, et al. (2002) Purification and functional characterization of SET8, a nucleosomal histone H4-lysine 20-specific methyltransferase. *Curr Biol* 12(13):1086–1099.
38. Imai Y, et al. (1999) The CED-4-homologous protein FLASH is involved in Fas-mediated activation of caspase-8 during apoptosis. *Nature* 398(6730):777–785.
39. van de Wetering M, Clevers H (1993) Sox 15, a novel member of the murine Sox family of HMG box transcription factors. *Nucleic Acids Res* 21(7):1669.
40. Fukuda MN, Sugihara K (2012) Trophinin in cell adhesion and signal transduction. *Front Biosci (Elite Ed)* 4:342–350.
41. Gao G, et al. (2003) NPAT expression is regulated by E2F and is essential for cell cycle progression. *Mol Cell Biol* 23(8):2821–2833.
42. Schwartz RA, et al. (2007) The Mre11/Rad50/Nbs1 complex limits adeno-associated virus transduction and replication. *J Virol* 81(23):12936–12945.
43. Lentz TB, Samulski RJ (2015) Insight into the mechanism of inhibition of recombinant adeno-associated virus by the Mre11/Rad50/Nbs1 complex. *J Virol* 89(1):181–194.
44. Wallen AJ, Barker GA, Fein DE, Jing H, Diamond SL (2011) Enhancers of adeno-associated virus AAV2 transduction via high throughput siRNA screening. *Mol Ther* 19(6):1152–1160.
45. High KA (2011) Gene therapy for haemophilia: A long and winding road. *J Thromb Haemost* 9(Suppl 1):2–11.
46. Chou JY, Mansfield BC (2011) Recombinant AAV-directed gene therapy for type I glycogen storage diseases. *Expert Opin Biol Ther* 11(8):1011–1024.
47. Jacobs F, Wang L (2011) Adeno-associated viral vectors for correction of inborn errors of metabolism: Progressing towards clinical application. *Curr Pharm Des* 17(24):2500–2515.
48. Ponder KP, Haskins ME (2007) Gene therapy for mucopolysaccharidosis. *Expert Opin Biol Ther* 7(9):1333–1345.
49. Grimm D, Kern A, Rittner K, Kleinschmidt JA (1998) Novel tools for production and purification of recombinant adenoassociated virus vectors. *Hum Gene Ther* 9(18): 2745–2760.
50. Grimm D, Kay MA, Kleinschmidt JA (2003) Helper virus-free, optically controllable, and two-plasmid-based production of adeno-associated virus vectors of serotypes 1 to 6. *Mol Ther* 7(6):839–850.
51. Gao G, et al. (2004) Clades of Adeno-associated viruses are widely disseminated in human tissues. *J Virol* 78(12):6381–6388.
52. Ayuso E, et al. (2010) High AAV vector purity results in serotype- and tissue-independent enhancement of transduction efficiency. *Gene Ther* 17(4):503–510.
53. Kronenberg S, Böttcher B, von der Lieth CW, Bleker S, Kleinschmidt JA (2005) A conformational change in the adeno-associated virus type 2 capsid leads to the exposure of hidden VP1 N termini. *J Virol* 79(9):5296–5303.

Supporting Information

Mano et al. 10.1073/pnas.1503607112

SI Materials and Methods

Cells. HeLa, U2OS, and MRC5 cell lines (ATCC) were maintained in DMEM 1 g/L glucose (Life Technologies) supplemented with 10% (vol/vol) FBS (Life Technologies) and antibiotics, in a 5% (vol/vol) CO_2, humidified atmosphere, at 37 °C. To obtain HeLa-EGFP, HeLa cells seeded on a 10-cm cell culture dish were transfected with the pEGFP-C1 plasmid (Clontech) using FuGENE HD Transfection reagent (Promega). After selection in culture medium with 400 μg/mL G418 (Life Technologies) for approximately 10 d, cells expressing high levels of EGFP were enriched by FACS sorting and propagated as a polyclonal cell population. Stock cultures of HeLa-EGFP (approximately 95% EGFP-positive cells) and HeLa/GFP-LacR cells were maintained in culture medium supplemented with 200 μg/mL or 400 μg/mL G418, respectively.

Production and Purification of Recombinant AAV Vectors. All of the AAV vectors used in this study were generated by the ICGEB AVU (www.icgeb.org/avu-core-facility.html). Briefly, AAV vectors were generated in HEK293 cells, using a dual-plasmid cotransfection procedure with pDG, pDF5, or pDF6 as helper plasmids for packaging vector genomes into AAV2, AAV5, and AAV6 capsids, respectively (49, 50), and a triple-plasmid cotransfection procedure for packaging into AAV9 capsids (51). Viral stocks were purified by PEG precipitation from clarified cell lysates and cell culture supernatant followed by two consecutive $CsCl_2$ gradient centrifugations, as described by Ayuso et al. (52). Full viral particles obtained from the gradient were extensively dialyzed in PBS and stored in aliquots at −80 °C until use. Titration of AAV vector particles was performed by real-time PCR quantification of the number of viral genomes, as described previously (31); the viral vector preparations used in this work were based on the AAV2 genome and had titers between 2.5×10^{10} and 5.5×10^{12} vg/mL. Transgene expression from all vectors was driven by the CMV IE promoter, with the exception of ssAAV8-ApoE/hAAT-EGFP, in which EGFP expression was under the control of the ApoE/hAAT promoter (33, 35). The plasmid encoding the genome for AAV2LacO.14 was described previously (32) The plasmid encoding the genome for scAAV2-EGFP was kindly provided by R. J. Samulski (University of North Carolina, Chapel Hill, NC).

The plasmid used to produce the ΔVP1-ssAAV2 particles was obtained by site-directed mutagenesis, using the following primers: ΔVP1 forward, 5′- CAATAAATGATTTAAATCAGGTTTGGCTGCCGATGGTTATCTTCC-3′ and ΔVP1 reverse, 5′- GGAAGATAACCATCGGCAGCCAAACCTGATTTAAATCATTTATTG-3′, which introduced a mutation in the start codon of VP1 protein from ATG to TTG (53); mutation was verified by sequencing, and absence of VP1 protein was confirmed by Western blot.

AAV Transduction. Transduction experiments with the different AAV vectors was performed at moi: 2,500 vg/cell (wild-type vectors) or 2.5×10^5 vg/cell (ΔVP1-ssAAV2 vectors). Analysis of AAV transduction was performed at 24 h after vector addition to the cells.

For the transduction experiments with AAV6 and AAV9, cells were treated with 50 mU/mL Neuraminidase (Neuraminidase from *Vibrio cholerae*; Sigma-Aldrich) for 3 h, before addition of the vectors.

Genome-Wide RNAi Screening. The genome-wide human siRNA library (siGENOME SMARTPool; pools of four siRNAs per gene) targeting 18,120 human genes, was obtained from Dharmacon, Thermo Scientific.

For the genome-wide siRNA screening in HeLa cells, siRNAs were transferred robotically from stock library plates to white 384-well plates (PerkinElmer); columns 1, 2, 23, and 24 were left empty for addition of controls (buffer, nontargeting control siRNA and siRNAs against luciferase and PLK1). siRNAs were transfected using a standard reverse-transfection protocol, at a final siRNA concentration of 50 nM. Briefly, the transfection reagent (Lipofectamine RNAiMAX; Life Technologies) was diluted in OPTI-MEM (Life Technologies) and added to the siRNAs arrayed on the 384-well plates; 30 min later, HeLa cells, suspended in culture medium without antibiotics, were seeded (2.0×10^3 per well). Forty-eight hours after transfection, cells were transduced with a recombinant ssAAV2 vector (ssAAV2-Luciferase; moi: 2,500 vg/cell) encoding for the Firefly luciferase reporter gene; 21 h later, Alamar Blue (Life Technologies) was added to the culture medium for 3 h. At 72 h after transfection (i.e., 24 h after transduction with ssAAV2-Luciferase), Alamar Blue fluorescence was measured (λ_{exc} = 530 nm; λ_{em} = 590 nm), and cells were immediately lysed and analyzed for luciferase activity. Conditions were optimized to achieve subsaturating levels of AAV transduction, to allow detection of both positive and negative regulators. Luciferase activity was measured using the PJK Beetle juice-glow reagent (PJK GmbH), according to the manufacturer's instructions. Alamar Blue and luciferase activity were measured using a PerkinElmer Envision multimode reader (PerkinElmer).

For the image-based secondary screenings, siRNA pools corresponding to the 1,483 genes selected from the primary screening were cherry-picked from siRNA library stock plates and rearrayed onto black clear-bottom 384-well plates (PerkinElmer); to minimize artifacts attributable to edge effects, the two outer columns and rows were left empty, and controls were added to columns 12 and 13 of each plate. Transfection was performed as described above for the genome-wide screening. For the AAV2 transduction experiments, HeLa-EGFP or HeLa cells were transduced 48 h after siRNA transfection with ssAAV2-DsRed or scAAV2-EGFP, respectively, at moi: 2,500 vg/cell. Cells were fixed at 72 h after plating (i.e., 24 h after AAV transduction) and processed for fluorescence microscopy. For the analysis of DNA damage in the absence of AAV transduction, HeLa cells were transfected as described above, fixed 48 h after transfection, and processed for immunofluorescence.

All screenings were performed in duplicate, at the ICGEB High-Throughput Screening Facility (www.icgeb.org/high-throughput-screening.html).

Fluorescence Staining and Immunofluorescence. For the AAV transduction experiments with ssAAV2-DsRed or scAAV2-EGFP and for the experiments with AAV2LacO.14, cells were fixed with 4% (wt/vol) paraformaldehyde (PFA) for 15 min, washed with PBS, and stained with Hoechst 33342 (Life Technologies).

For evaluation of DNA damage, cells were fixed with 4% PFA for 15 min and permeabilized with 0.5% Triton X-100 in PBS for 10 min, followed by 30 min of blocking in 1% BSA (Roche). Cells were then incubated for 1 h with a primary antibody for Phospho-Histone-H2A.X p-Ser139 (ɣ-H2AX) (05-636; 1:500 in blocking solution; Millipore). Cells were washed with PBS and incubated for 1 h with an Alexa Fluor-488–conjugated secondary antibody

(Life Technologies) and stained with Hoechst 33342 (Life Technologies).

Image Acquisition and Analysis. For the image-based secondary screenings, image acquisition was performed using an ImageXpress Micro automated high-content screening fluorescence microscope (Molecular Devices) at a 10× magnification; a total of four images were acquired per wavelength, well, and replicate, corresponding to approximately 1,500–2,000 cells analyzed per condition and replicate. Image analysis was performed using the Multi-Wavelength Cell Scoring application module implemented in MetaXpress software (Molecular Devices). Quantification of cells positive for ɣ-H2AX was performed using the same methodology, except that nine images were acquired per well, at a 20× magnification.

For the analysis of single-stranded to double-stranded genome conversion, image acquisition was performed in a Zeiss LSM-510 confocal laser-scanning microscope at a 63× magnification. Cells were scored manually for the presence of GFP-LacR foci.

Sections of mouse liver were imaged using an ImageXpress Micro automated high-content screening fluorescence microscope, at a 4× magnification. Images of large tissue areas (36 images per sample) were obtained by stitching of individual images, using MetaXpress software; quantification of EGFP intensity in tissue samples was performed using the MetaXpress software.

Functional Gene Analysis. Functional analysis of the genes identified in the primary screening as required or inhibitory to AAV transduction was conducted using Ingenuity Pathway Analysis software (IPA) (Ingenuity Systems). Datasets were uploaded into IPA and analyzed for functional enrichment in terms of Molecular and Cellular Functions, based on the information in the Ingenuity Knowledge Base. Enrichments were calculated by IPA using right-tailed Fisher's exact test; uncorrected *P* values are shown.

Cell Cycle Analysis. For cell cycle analysis by flow cytometry, cells were fixed as described above and washed with PBS. DNA staining was performed by incubating cells with 50 μg/mL propidium iodide (Sigma) and 0.2 mg/mL RNase A (Sigma) in buffer H (20 mM Hepes, 160 mM NaCl, 1 mM EGTA), for 30 min at 37 °C. Cells (10,000 cells per experimental condition and replicate) were analyzed on a FACSCalibur flow cytometer (Becton Dickinson); analysis of the distribution of the different phases of cell cycle was performed using the FlowJo software (Tree Star) with the Dean–Jett–Fox model.

Whole-Cell Protein Extracts and Western Blot. For Western blot analysis, HeLa cells were seeded in six-well plates (2.0×10^5 per well). Transfection of siRNA pools was performed using Lipofectamine RNAiMAX, at a final siRNA concentration of 50 nM.

Forty-eight hours after siRNA transfection, the cells were collected in HNNG buffer [15 mM Hepes (pH 7.5), 250 mM NaCl, 1% Nonidet P-40, 5% (vol/vol) glycerol, 1 mM PMSF] supplemented with 25 mM NaF, 10 mM β-glycerophosphate, 0.2 mM sodium orthovanadate, and protease inhibitors (Roche). Protein concentration was determined by the colorimetric bicinchoninic acid protein assay (Thermo Scientific) in a Envision multimode reader. Protein samples (15 μg) were separated in 8–12% SDS/PAGE minigels and transferred onto nitrocellulose membranes (GE Healthcare). Membranes were blocked in 5% (wt/vol) BSA in TBST [50 mM Tris·HCl (pH 7.4), 200 mM NaCl, 0.04% Tween 20] at room temperature for 2 h; membranes for P-NBS1 were blocked overnight in 5% (wt/vol) nonfat dry milk; immunoblots for NBS1, P-CHK1, ATM, CHK1, α-tubulin and HSP70 were blocked in 5% nonfat dry milk at room temperature for 2 h. The following primary antibodies were used: SETD8 (C18B7; 1:500; Cell Signaling), NPAT (ab70595; 1:500; Abcam), Phospho-ATM p-Ser1981 (P-ATM) (4526; 1:500 in 5% BSA; Cell Signaling), ATM (2873; 1:500 in 5% BSA; Cell Signaling), Phospho-NBS1 p-Ser343 (P-NBS1) (NB100-92610; 1:500 in 5% nonfat dry milk; Novus Biologicals), NBS1 (NB100-143; 1:3,000 in 5% nonfat dry milk; Novus Biologicals), Phospho-CHK1 p-Ser345 (P-CHK1) (2348; 1:500 in 5% BSA; Cell Signaling), CHK1 (2360; 1:1,000 in 5% nonfat dry milk; Cell Signaling) and α-tubulin (T5168; 1:10,000 in 5% nonfat dry milk; Sigma). For analysis of AAV vector particles, an anti-AAV VP1/VP2/VP3 mouse monoclonal antibody was used (B1; 1:200; Progen Biotechnik). Secondary antibodies coupled to horseradish peroxidase (Santa Cruz Biotechnology) were used. Signals were detected using the ECL chemiluminescence system (Amersham).

HU (Sigma) was used a positive control in these experiments; where indicated, cells were incubated overnight with 1 mM HU, before cell fixation.

AAV Liver Transduction. Juvenile mice (CD1; 1-mo old; $n = 3$–5 per group) were injected into the portal vein with a mixture of transfection reagent (Lipofectamine RNAiMAX) and each of the siRNA pools against the top 10, or a nontargeting control (1:1 transfection reagent:siRNA mixture, 25 μL), together with AAV8-ApoE/hAAT-EGFP at a dose of 5×10^{10} vg (25 μl); a volume of 50 μL per animal was injected slowly using a U-100 insulin syringe. Animals were killed 10 d or 5 wk after injection to evaluate AAV transduction. Livers were collected, carefully divided in lobes, and a piece of every lobe was processed for evaluation of the percentage of transduced cells by fluorescent microscopy, or quantification of EGFP expression, by real-time qPCR.

For fluorescent microscopy, liver tissue was fixed in 4% PFA overnight at 4 °C, cryoprotected in 30% (wt/vol) sucrose overnight at 4 °C, and then frozen at −20 °C. Liver sections (5 μm) were imaged using an ImageXpress Micro automated high-content screening microscope equipped with a 4× objective. Nuclei were identified by counter staining sections with DAPI (Life Technologies); slides were mounted in Vectashield mounting medium (Vector Labs).

RNA Isolation and Quantitative Real-Time PCR. Total RNA from liver tissue or cells treated with the different siRNA pools was isolated using TRIzol (Life Technologies). mRNA was reverse-transcribed using random primers (Life Technologies) and M-MLV reverse transcriptase (Life Technologies). Real-time quantitative analysis was performed using the iQ SYBR Green Supermix or iQ Supermix, in a CFX96 Real-Time system (Bio-Rad). The following primers were used: GFP-forward, 5′-TCAAGGAGGACGGCAACATC-3′; and GFP-reverse, 5′-TTGTGGCGGATCTTGAAGTTC-3′. For the evaluation of gene knockdown, analysis was performed 48 h after siRNA transfection, using the following Taqman assays (Life Technologies): SETD8, Hs01029945_m1; CASP8AP2, Hs01594281_m1; SOX15, Hs00199511_m1; TROAP, Hs00193896_m1; NPAT, Hs00159638_m1; PHC3, Hs00227887_m1; CHAF1A, Hs00193920_m1; SF3B1, Hs00961640_g1; RTBDN, Hs01564130_m1; and WWC2, Hs00420500_m1. Results were normalized to GAPDH [TaqMan assays 4352339E (mouse) and 4326317E (human); Life Technologies]. Fold changes were determined using the $2^{-\Delta\Delta Ct}$ method.

Statistical Analysis. Unless otherwise indicated, all data are presented as means ± SEM. Statistical analysis was carried out using Prism Software (GraphPad). For statistical comparison of two groups, two-tailed Student's *t* test was used. A value of $P < 0.05$ was considered significant.

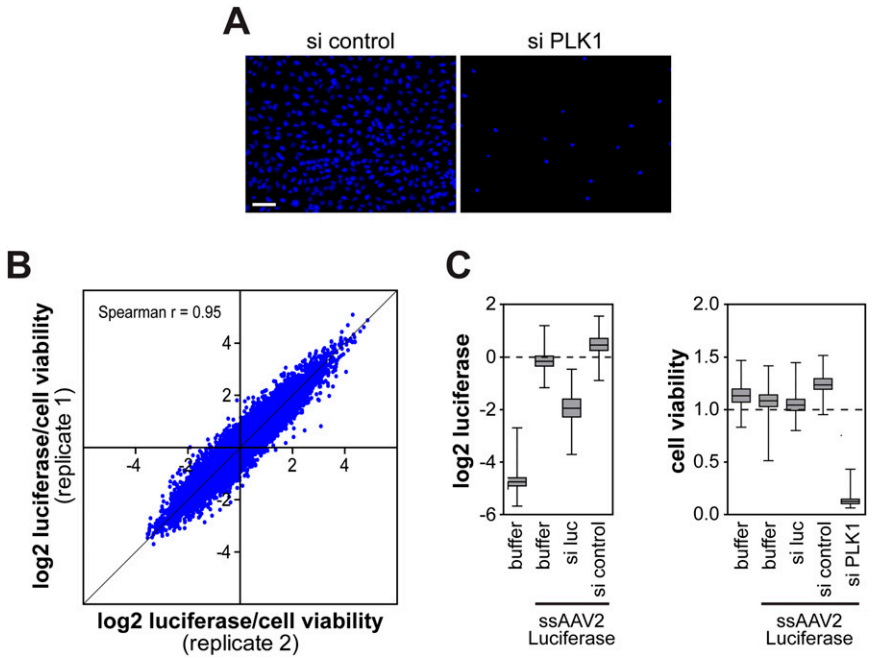

Fig. S1. Genome-wide siRNA screening for AAV transduction. (*A*) Representative images of HeLa cells transfected with control or a toxic siRNA (siRNA against PLK1), at 48 h after transfection. (Scale bar: 100 μm.) (*B*) Correlation between the two replicates of the primary screening, using a genome-wide library of siRNA targeting 18,120 genes. Results are shown as fold change of AAV transduction normalized to cell viability, in log2 scale; Spearman rank correlation coefficient between the two replicates is shown. (*C*) Summary of screening controls, included in all of the screening plates. (*Left*) Effect of control siRNAs on luciferase activity. (*Right*) Effect of control siRNAs on cell viability. Whiskers in the graphs represent minimum and maximum.

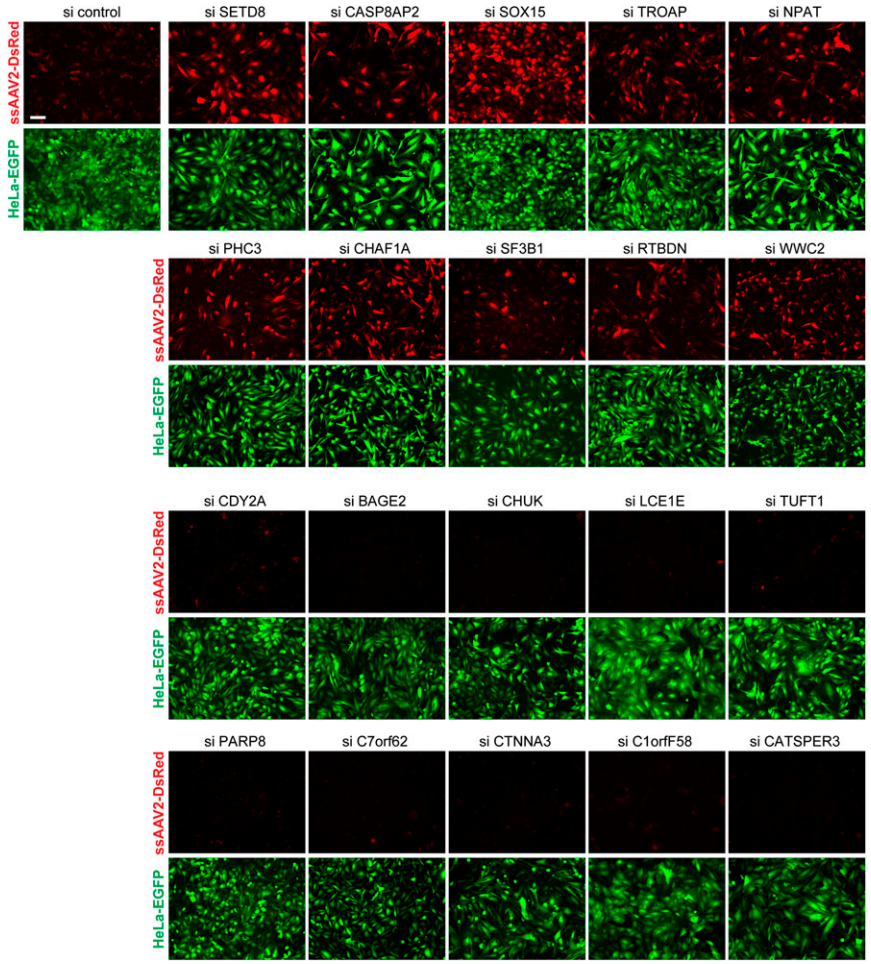

Fig. S2. Effect of siRNAs on AAV transduction. Representative images of HeLa-EGFP cells treated with the 10 siRNA pools that increased (upper images) or decreased (lower images) AAV transduction more efficiently in the primary screening. HeLa-EGFP cells were transfected with the siRNAs and transduced 48 h later with ssAAV2-DsRed, at moi: 2,500 vg/cell; AAV transduction was analyzed after 24 h. (Scale bar: 100 μm.)

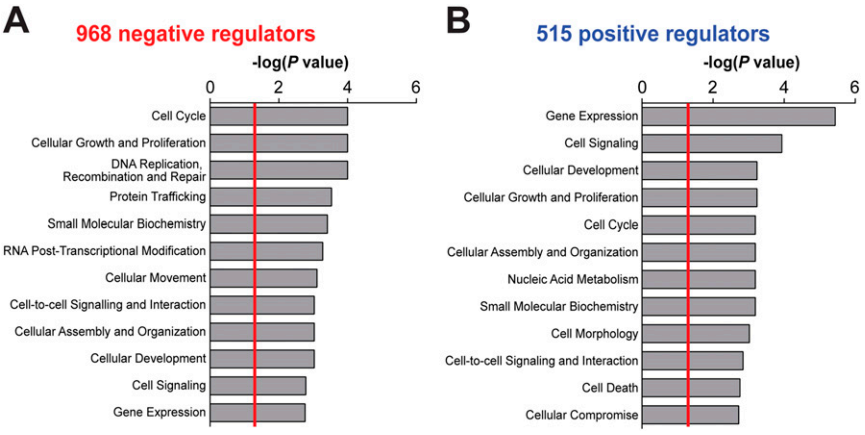

Fig. S3. Functional analysis of genes identified in the genome-wide siRNA screening. (*A* and *B*) Functional categories enriched among the 968 genes identified in the primary screening as negative regulators of AAV transduction (*A*) or 515 genes identified as positive regulators (*B*). Enrichment analysis was performed using IPA software; the 12 most enriched categories are shown. Red line represents $P = 0.05$.

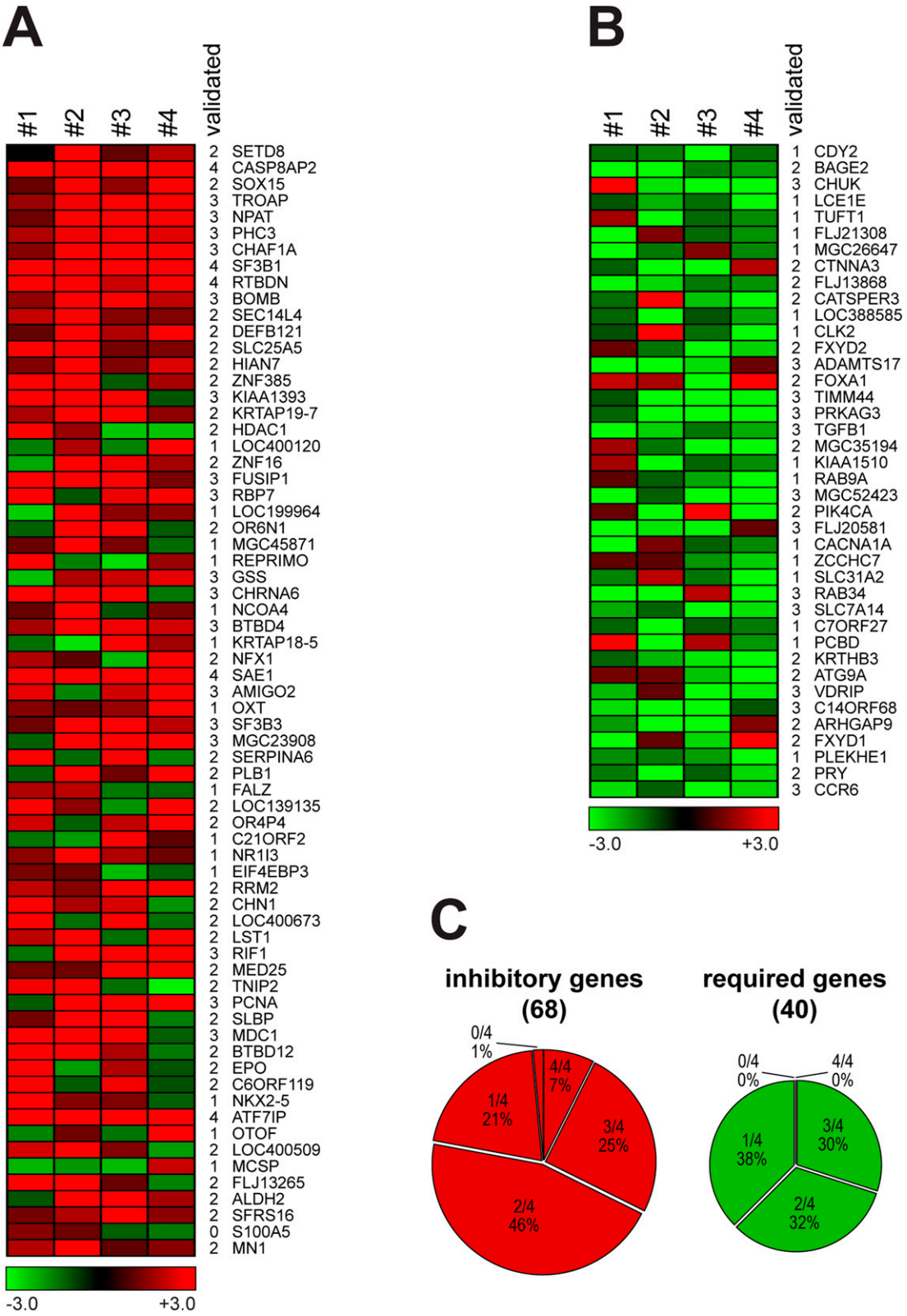

Fig. S4. Deconvolution of selected siRNA pools. (*A* and *B*) Effect of individual siRNAs on AAV transduction. The four individual siRNAs corresponding to the siRNA pools exhibiting the strongest effects were tested: 68 inhibitory genes (*A*); 40 required genes (*B*). HeLa cells were transfected with the siRNAs and transduced 48 h later with ssAAV2-luciferase, at moi: 2,500 vg/cell; AAV transduction was analyzed after 24 h. Heat map represents fold change of AAV transduction normalized to control siRNA. (*C*) Percentage of siRNA pools validated with zero, one, two, three, or four of the four siRNAs tested per gene.

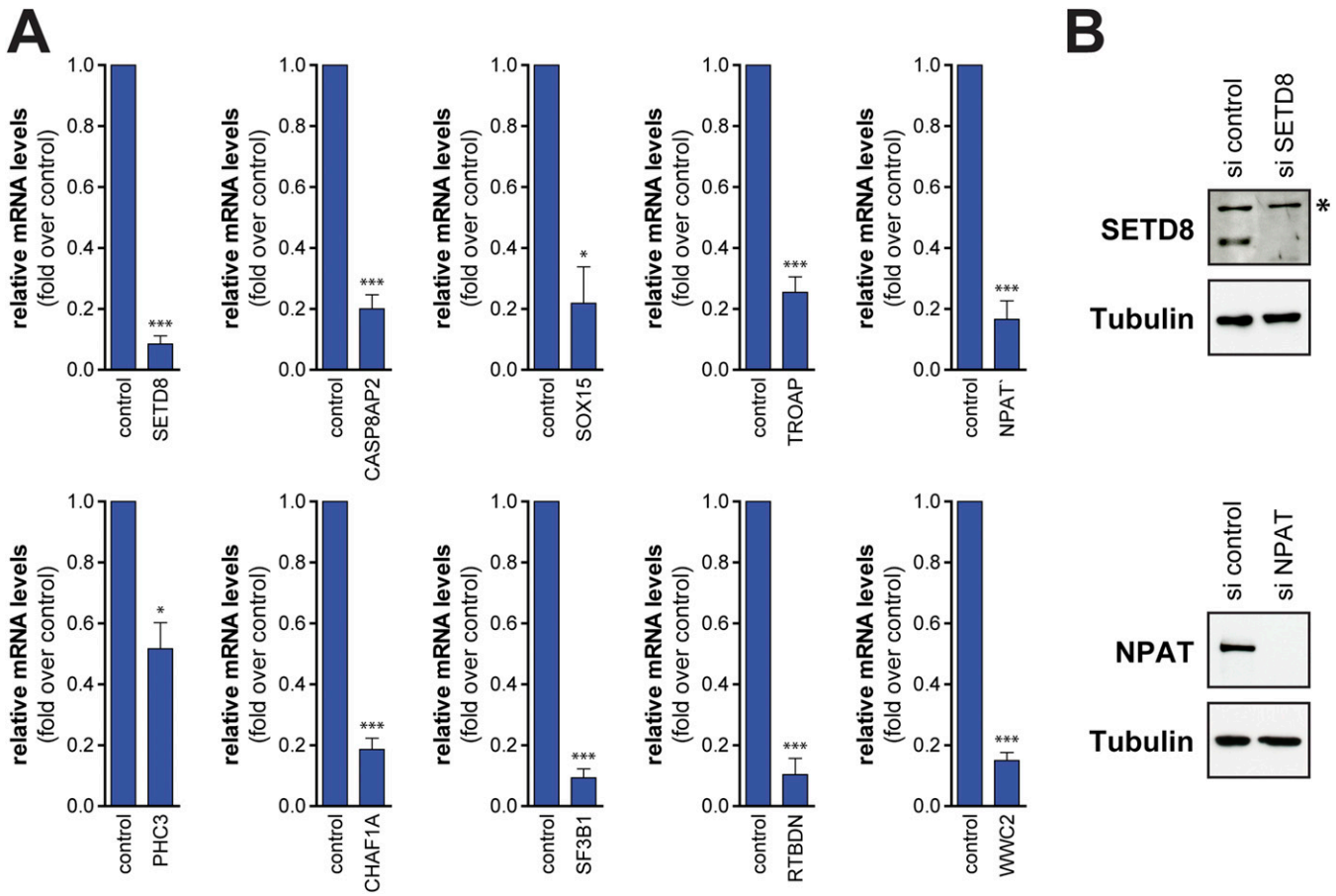

Fig. S5. Efficiency of knockdown by siRNAs. (*A*) Effect of the siRNA pools against the top 10 siRNAs increasing transduction in the primary screening on target transcript levels. Results were normalized to GAPDH and are shown as means ± SEM ($n = 3$). *$P < 0.05$ and ***$P < 0.001$. (*B*) Western blot analysis of the effect of the siRNA pools against SETD8 and NPAT on the protein levels. Asterisk on upper blot denotes a nonspecific band, as per the antibody datasheet; tubulin was used as a loading control.

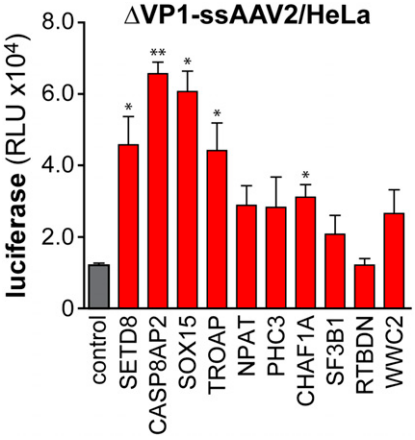

Fig. S6. Efficiency of siRNAs on δVP1 AAV transduction. Effect of the siRNA pools against the top 10 siRNAs increasing transduction in the primary screening on the transduction mediated by δVP1-ssAAV2 particles. The δVP1-ssAAV2 particles are strongly impaired in intracellular trafficking because of the lack of the capsid protein VP1. Results are shown as means ± SEM ($n = 3$). *$P < 0.05$ and **$P < 0.01$.

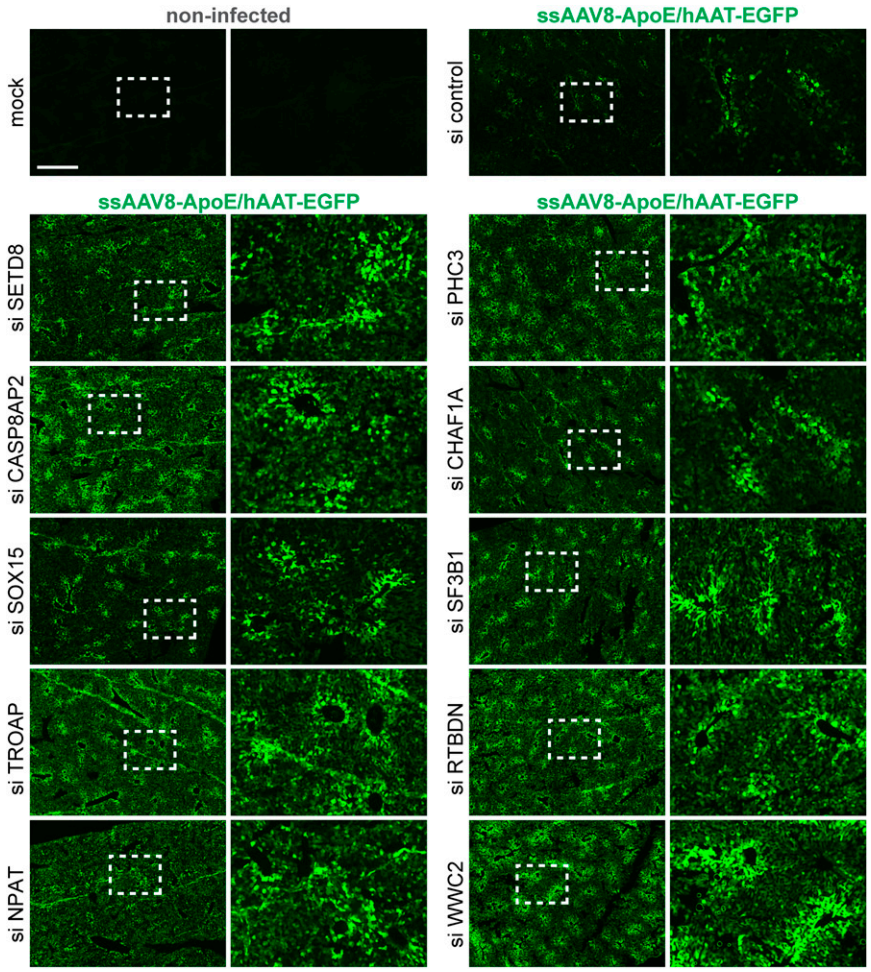

Fig. S7. Effect of siRNAs on AAV transduction in vivo. Representative images of liver sections of animals treated with control and selected siRNAs (top 10 siRNAs increasing transduction in the primary screening) and transduced with AAV8 encoding EGFP (ssAAV8-ApoE/hAAT-EGFP). siRNA pools formulated with a commercial transfection reagent were delivered together with ssAAV8-ApoE/hAAT-EGFP (5×10^{10} vg) by portal vein injection and analyzed 10 d after injection. (Scale bar: 1 mm.)

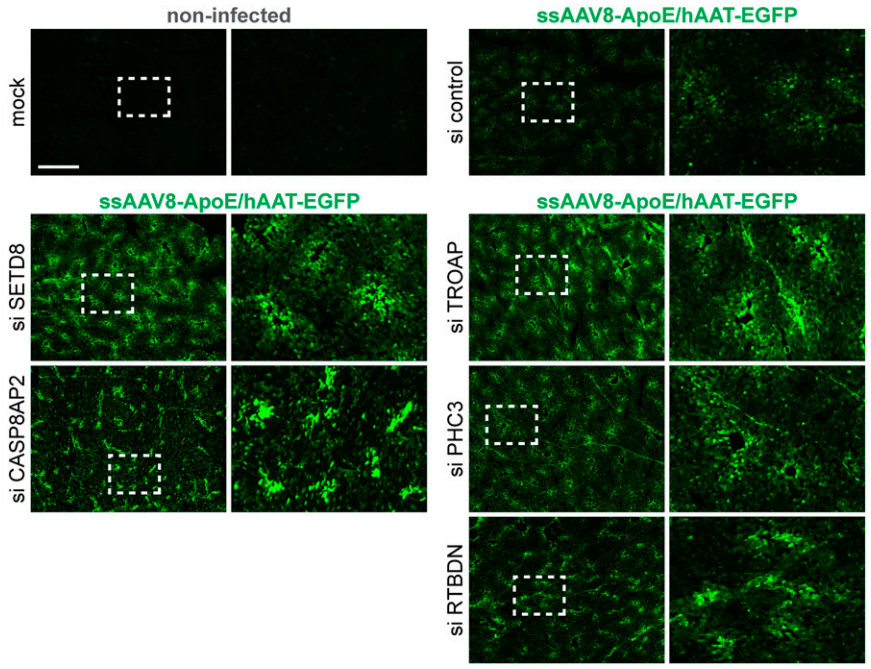

Fig. S8. Effect of siRNAs on AAV transduction in vivo. Representative images of liver sections of animals treated with control and selected siRNAs from the top 10 siRNAs increasing transduction in the primary screening and transduced with AAV8 encoding EGFP (ssAAV8-ApoE/hAAT-EGFP). siRNAs targeting two proteins that induce DNA damage (SETD8 and CASP8AP2) and three proteins that have no implications to DNA damage (TROAP, PHC3, and RTBDN) were selected. siRNA pools formulated with a commercial transfection reagent were delivered together with ssAAV8-ApoE/hAAT-EGFP (5×10^{10} vg) by portal vein injection and analyzed 5 wk after injection. (Scale bar: 1 mm.)

Table S1. Effect of selected siRNAs on AAV transduction

Gene identification no.	Gene symbol	Gene name	Fold change AAV2
387893	SETD8	SET domain containing (lysine methyltransferase) 8	51.4
9994	CASP8AP2	caspase 8-associated protein 2	30.2
6665	SOX15	SRY (sex-determining region Y)-box 15	27.0
10024	TROAP	trophinin-associated protein (tastin)	25.1
4863	NPAT	nuclear protein, ataxia-telangiectasia locus	23.6
80012	PHC3	polyhomeotic homolog 3 (*Drosophila*)	23.1
10036	CHAF1A	chromatin assembly factor 1, subunit A (p150)	20.9
23451	SF3B1	splicing factor 3b, subunit 1, 155 kDa	20.5
83546	RTBDN	Retbindin	19.3
80014	WWC2	WW and C2 domain-containing 2	19.2
9426	CDY2A	chromodomain protein, Y-linked, 2A	−11.7
85319	BAGE2	B melanoma antigen family, member 2	−10.6
1147	CHU.K.	conserved helix–loop–helix ubiquitous kinase	−10.1
353135	LCE1E	late cornified envelope 1E	−9.8
7286	TUFT1	tuftelin 1	−9.7
79668	PARP8	poly(ADP ribose) polymerase family, member 8	−9.4
219557	C7orf62	chromosome 7 ORF 62	−9.1
29119	CTNNA3	catenin (cadherin-associated protein), α3	−9.1
64755	C16orf58	chromosome 16 ORF 58	−9.0
347732	CATSPER3	cation channel, sperm-associated 3	−8.9

Average results from the two screening replicates for the top 10 negative and positive regulators of AAV transduction.

Dataset S1. Genome-wide siRNA screening for AAV transduction: primary screening data

Dataset S1

Dataset S2. Percentage of DsRed- and EGFP-positive cells after treatment with siRNAs against the 1,483 genes selected from the primary screening

Dataset S2

Dataset S3. Effect of the knockdown of the 1,483 selected genes on the percentage of cells transduced with ssAAV2-DsRed or scAAV2-EGFP vectors

Dataset S3

Dataset S4. Effect of knockdown of the 1,483 selected genes affecting AAV transduction on the percentage of cells presenting cellular DNA damage, revealed by the presence of γ-H2AX foci

Dataset S4